Exp. Brain Res. 16, 161—183 (1972)

The Facial Nucleus of Cat: Antidromic and Synaptic Activation and Peripheral Nerve Representation[1,2]

S. T. Kitai, T. Tanaka[3], N. Tsukahara[4] and H. Yu[5]

Morin Memorial Laboratory, Department of Anatomy, School of Medicine, Wayne State University, Detroit (USA)

Received March 11, 1972

Summary. The facial nucleus (FN) of the cat was studied by electrophysiological method for (1) general characteristics of the FN neurons during antidromic activation, (2) topographical representation of the peripheral branches of the facial nerve and (3) synaptic activities induced in the FN neurons following peripheral facial nerve stimulation.

Stimulation of either peripheral branches or the genu of the facial nerve produced negative field potential of 2—3 mV in the FN. The field potential had a latency of less than 1 msec, refractory period of 2—3 msec and a relatively short duration. During double shock testing of the antidromic field potentials, the test potentials were suppressed (after initial recovery from the refractory period) for a duration of up to 80—100 msec.

Intracellular analysis revealed that antidromic firing of the FN neuron is composed of M, IS, SD spikes. The rise time of spike potentials ranged from 0.23 msec to 0.53 msec and fall time 0.73 msec to 4.7 msec. The duration of the spike after-hyperpolarization varied from 6 msec to 60 msec with latencies to peak of 1.5 msec to 14 msec. Double shock testing showed that the summation effect of the afterhyperpolarization was greater at shorter time intervals. The latencies of the spike potentials varied from 0.46 msec to 1.1 msec for peripheral nerve stimulation and 0.18 msec to 1 msec for genu stimulation. The conduction velocity of the facial nerve ranged from 25 m/sec to 75 m/sec. These results were compared with the known characteristics of other cranial and spinal motoneurons.

Topographical representation of the peripheral branches of the facial nerve was that the PA was represented solely in the medial aspect, TZ mainly in the dorsal aspect of the intermediate portion and BL in the ventral aspect of the intermediate and mainly in the lateral aspect of the nucleus.

---

1 This study was supported by U.S. Public Health Service Grants NB 00405 and RR 5384.

2 Based, in part, upon a dissertation submitted to the Department of Anatomy in partial fulfilment of the degree of Ph. D. awarded to H. Yu. Dr. Yu was a recipiant of a fellowship from the Charles B. deVlieg Foundation.

3 Present addres of T. Tanaka is: Department of Physiology, Mie Prefectural University, School of Medicine, Tsu, Mie-ken, Japan.

4 Present address of N. Tsukahara is: Department of biophysical Engineering, Faculty of Engineering Science, Osaka University, Toyonaka, Japan.

5 Present address of H. Yu is: Institute for Dental Research, University of Michigan, School of Dentistry, Ann Arbor, Michigan.

Stimulation of peripheral facial nerve produced negative field potentials in the FN or induced EPSPs in the FN neurons with latencies of 4—7 msec. The synaptic inputs were found mainly in the medial aspect of the FN by PA stimulation. These synaptic inputs were discussed as being relayed through the trigeminal nucleus.

Key words: Facial nucleus — Topographical representation — Cat

Introduction

The facial nucleus (FN) of the cat is a round, well-circumscribed nuclear mass situated ventrolaterally in the pontine-medullary junction and extends from a level of the inferior pole of the superior olivery nucleus to the superior pole of the inferior olivary nucleus (Papez, 1927; and Van Buskirk, 1945). The cell size varies from the small cells (16—20 μ) to the medium (20—35 μ) and to the large (40—60 μ) (Van Buskirk, 1945). The FN is grouped into four (i. e. dorsomedial, ventromedial, intermediate and lateral) (Courville, 1966) to six (i. e. medial, ventromedial, intermediate, dorsal, lateral and ventrolateral) (Papez, 1927) subdivisions based on the morphological criteria.

Correlation of subdivision of the nucleus with the peripheral branches of the facial nerve was obtained by studying retrograde chromatolytic changes in the nucleus (Courville, 1966; Papez, 1927; Vraa-Jensen, 1942). Inspite of some discrepancies among the studies, it could be summarized that the medial group is related to the posterior auricular, the intermediate to the temporal- and zygomatoorbital and the lateral to the superior and inferior buccolabial branch.

Even though many detailed anatomical (Bruesch, 1944; Courville, 1966; Foley and DuBois, 1943; Huber and Hughson, 1926; Pearson, 1947; Ramón y Cajal, 1909; Rhinehart, 1918; Szentágothai, 1948; VanBuskirk, 1945; Vraa-Jensen, 1942), clinical and/or behavioral (Carmichael and Woollard, 1933; Davis, 1923; Kugelberg, 1952; Langworth and Taverner, 1963; Woody and Brozek, 1969) studies of the FN are available for various species, electrophysiological study of this nucleus is limited. Eletrical activities of the facial neurones to facial reflex (Lindquist and Martensson, 1970) or blink reflex (Woody and Brozek, 1969; Woody and Brozek, 1969) mechanism and facial nerve and muscle activities to blink reflex (Lindquist, 1970) have been reported. The findings on the intracellular and field potential analysis of the facial motoneurons to antidromic (Kitai *et al.*, 1971) and some orthodromic inputs from the spinal cord, the trigeminal complex (Christensen *et al.*, 1972; and Tanaka *et al.*, 1971) and the red nucleus (Yu *et al.*, 1972) have been preliminarily reported.

In this paper, the activity of the facial motoneurons following the facial nerve stimulation as recorded by intracellular and extracellular technique will be reported. Attempts are made to analyze (1) the general characteristics of the FN neurons during antidromic activation. (2) topographical representation of the peripheral branches of facial nerve and (3) some synaptic activities induced in the FN neurons following the peripheral facial nerve stimulation.

Methods

General Procedure

Experiments were performed on thirty-four cats, weighing between 2 and 4 kg. Animals were initially anaesthetized with sodium pentobarbital (40 mg/kg), injected intraperitoneally and later supplemented by intravenous injections. In addition, during recording, muscular movements were eliminated by gallamine injection (initial dose of approximately 2.5 mg — 5 mg/kg) with the animal artificially respirated.

Extensive craniotomy was performed to allow insertion of the stimulating and recording electrodes into the brain. In order to approach the facial nucleus and genu of the facial nerve from the dorsal direction, the overlying occipital cortex and the bony tentorium were removed. The dorsal portion of the cerebellum overlying the brain stem was also suctioned out. The wall of the cavity thus created in the cerebellum was lined firmly by a strip of photographic film so as to prevent the bleeding and deformation of the cavity. A heating pad was used to maintain the body temperatures between 36° C and 38° C. The temperature and the EKG of the animal were monitored all through the experiment.

Stimulation

FN neurons were activated either by stimulation of the peripheral branches or the genu of the facial nerve. For stimulation at the peripheral sites, the facial nerve was exposed distal to the stylomastoid foramen and the branches of the nerve were dissected out. The branches isolated were the posterior auricular (PA), temporal-zygomatico-orbital (TZ) and both superior and inferior buccolabial (BL) branches. The cut-end of each branch was stimulated in an electrode assembly, consisting of a pair of Ag-AgCl, rings in a plastic sleeve. The entire assembly was secured onto adjacent musculature.

For stimulation of the genu of the facial nerve, a concentric bipolar electrode with outside diameter of 300 μ was inserted stereotaxically. In some cases, to insure the placement in the genu, the position of the stimulating electrode was adjusted by monitoring the evoked potentials following stimulation of the peripheral branches of the facial nerve. In this manner, the threshold for the activation of the peripheral nerve branches could also be obtained. In other cases, where peripheral branches were not dissected, the positioning of the stimulating electrode inserted stereotaxically in the genu was adjusted by observing for maximum twitch responses in the face or temporal-auricular regions.

Stimuli to the genu, as well as to the peripheral branches, consisted of brief isolated current pulses of 0.05—0.1 msec duration delivered from a stimulator (Digimeter Device). At the termination of the experiment, the stimulation site in the genu was marked by passing a current of 0.5—1 mA through a center pole of the concentric electrode and identified by histological method.

Recordings

For the extracellular field potential analysis, glass microelectrodes filled with 3—4M NaCl solution with d—c resistance of 2 through 5 MΩ were used. Intracellular recordings were obtained by 3M KCl-filled glass electrodes with d—c resistance of 10—25 MΩ. The microelectrode was driven in vertically from the dorsal portion of the brain by a micromanipulator. For depth-profile field potential analysis of the FN, a recording microelectrode was first inserted through the nucleus to a depth where antidromic activities were no longer detected and the antidromic field potentials at various depths were recorded as the electrode was withdrawn to the point where they were no longer detectable.

The signals were recorded with a d—c coupled unity-gain cathode follower and displayed at two different gains (high gain for RC coupled amplifier with a time constant of 2 sec; low gain for DC recording) in an oscilloscope (Tektronix Model 565). The resting potentials of the cells were simultaneously monitored by a DC pen-recorder. At the end of recording, the microelectrode was cut so that the fine shaft remained in the nucleus. When the field analysis was done with several recording tracts in the nucleus, a number of the recording electrodes were cut and left in the nucleus for precise identification of recording tracts.

At the termination of the experiment, the animal was perfused through the heart with 10% formalin solution. The brain stem was sectioned by 80 μ thickness for identification of the stimulating electrodes and 60 μ for recording electrodes. In some cases, serial sections were

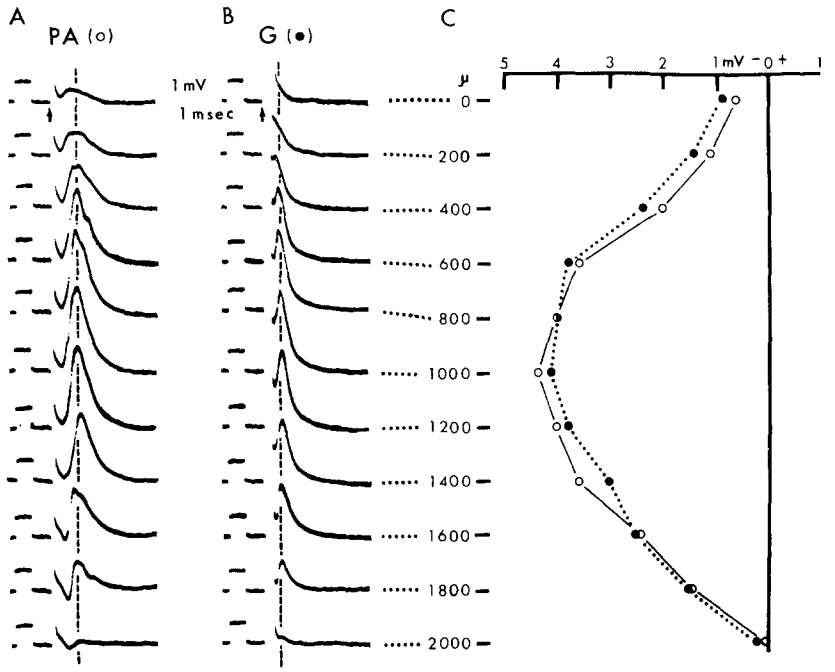

Fig. 1. *The depth profiles of field potentials evoked by PA and genu stimulation recorded in the FN are in A and B.* Time and voltage calibration at the beginning of each trace is 1 msec and 1 mV. The onset of stimulation is indicated by upward arrows in each top trace. All upward arrows in the subsequent figures indicate stimulus onset. In C, amplitudes and polarities of PA evoked (open circle) and genu evoked (closed circle) field potentials indicated by the vertical dotted lines in A and B are plotted in ordinate for the depths indicated on the abscissa

stained by cresyl violet for histological examination of the electrode tracts (Fig. 2A—D) and in others unstained sections were examined under a projection microscope.

Results

Field Potentials in the FN Induced by Antidromic Activation of Facial Motoneurons

When a recording microelectrode was inserted into the FN (see Fig. 2), short latency negative waves of a few milivolts were recorded following stimulation of either peripheral branches or the genu of the facial nerve. Figure 1A shows samples of depth profile of the field potentials recorded by withdrawing electrodes by 200 μ steps for a distance of 2 mm in a region of FN following stimulation of the PA. In the dorsal region, responses were small slow negativity with a latency of approximately 0.7 msec and duration of 3 msec with a latency to the peak of 1.7 msec. A few hundred microns in the nucleus, the amplitude of this negative wave increased significantly (i. e. at 600 μ) without appreciable changes in its latency. Though not prominent in this depth profile analysis, a small positive wave with a latency of 0.5 msec preceeding this negativity was sometimes detected (Kitai *et al.*, 1971). Also noted was a presence of rippling in the falling phase of negative wave indicating some differences in the rate of depolarization of the FN neurons. The peak amplitude of the negative wave was obtained at around 800 μ

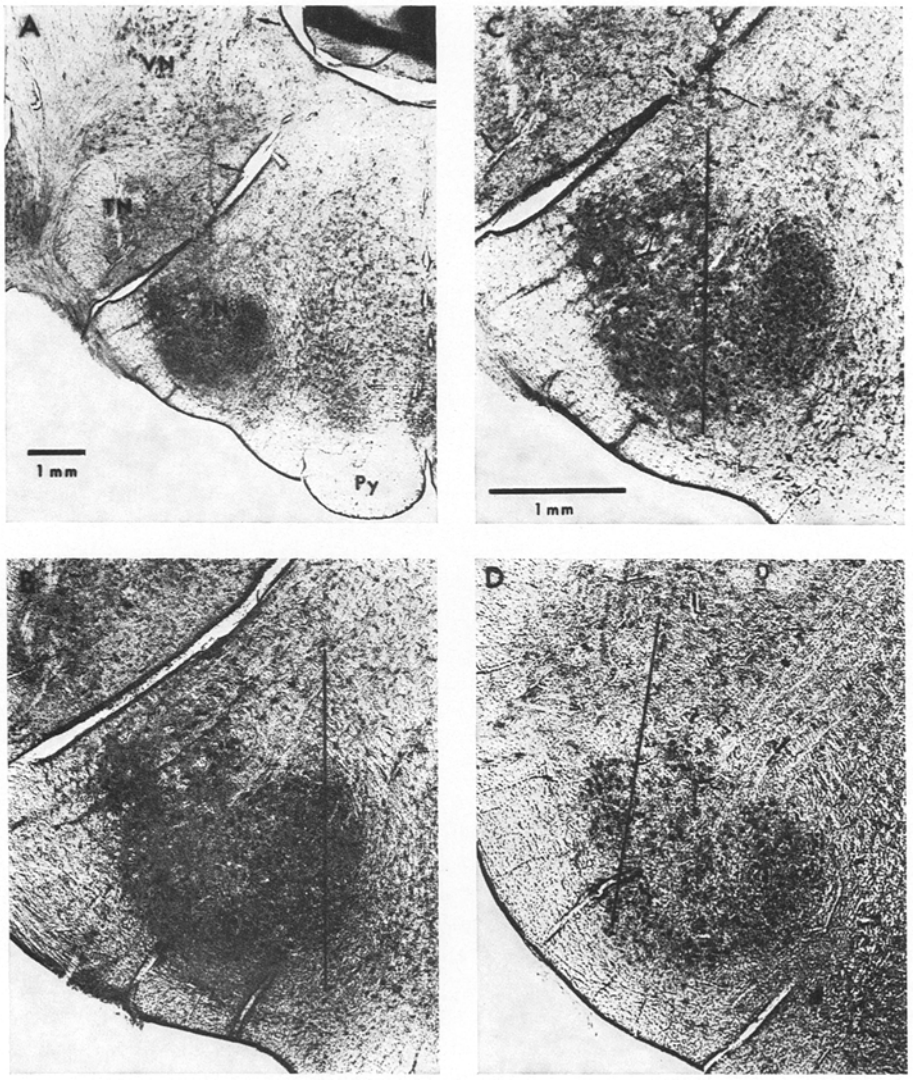

Fig. 2. *Photomicrograph of the regions of the facial nucleus for the histological identification of electrode tracts.* Scarring produced in the tissue by electrodes are indicated by arrows in A and C. Dark vertical line in B, C, D indicates electrode penetration (traced from scarring) for field potential analysis. The calibration in C also refers to B and D. VN: Vestibular nucleus, TN: Trigeminal nucleus, Py: Pyramid, FN: facial nucleus. Shrinkage of the tissue estimated to be about 30%

through 1200 μ depth. As the electrode was nearing the ventral limit of the nucleus, the amplitude of the negativity decreased; and in some cases, reversed to a small positivity (Kitai *et al.*, 1971). Figure 1B shows a concurrent depth analysis to stimulation at the genu of the facial nerve recorded from the corresponding locations to those in Fig. 1A. Even though there were some differences in the latencies and the duration of the negative waves, patterns of amplitude changes of the

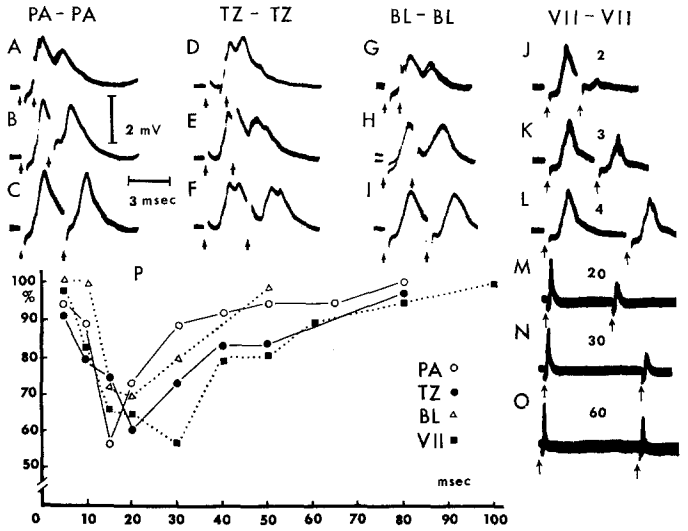

Fig. 3. *Antidromic field potentials in FN by double stimulation of PA* (A—C), TZ (D—F), BL (G—I) and of the entire stalk of the facial nerve (VII) distal to the stylomastoid foramen (J—O). In VII—VII, number above each records refer to time interval between shocks. Note that antidromic potentials are almost fully recovered at 3 msec (C, F, I) or the 4 msec (L) after the conditioning stimulus. Note also in M—O that the test responses were again suppressed by the conditioning after the initial recovery. Subsequent to the initial recovery, amplitude change of test antidromic field potential from the control value (100%) is plotted in ordinate as a function of time intervals in milliseconds between the conditioning and test stimuli in abscissa for PA (open circle), TZ (closed circle), BL (open triangle) and VII (closed square)

negative wave, in general, paralleled those activated by PA stimulation. These phenomena are graphically represented in Fig. 1 C. Considering their short latencies and other criteria tested for the identification of antidromic invasion (i. e. graded phenomena, short refractoriness, correlation with intracellular recordings), these negative waves were attributed to the antidromic activation of the FN neurons and were produced by summation of action currents.

In order to demonstrate a graded nature of these negative waves, the intensities of the antidromic stimulus were gradually changed from the level of threshold of the negative waves to several times that of the threshold. The maximum amplitude of the negative wave was attained by the stimulus intensity of about 2 times threshold for PA, 5 times for BL and TZ. Also noted was an appearance of additional depolarization after the peak of the negative wave and shortening of latencies with increase in stimulus intensities.

The refractoriness of FN neurons activated by PA, TZ, BL and the whole VIIth nerve stimulation was studied by a double shock technique and the sample records are shown in Fig. 3 A—L. The absolute refractoriness for all the branches tested were within one millisecond and the recovery of the test response to the control level was around 3 msec (Fig. 3 A—I). The negative waves evoked by TZ stimulation had two distinct inflections. The second inflection had a longer refractory period than the initial inflection but both negativities recovered almost to the initial level in around 3 msec. The late inflection thus signifies a difference

in a rate of depolarization of FN neurons (and may be due to a difference in caliber of nerve fibers). The inflections in the falling phase of the negative waves were found to be more prevelant in the potential activated by TZ or BL stimulation than by PA (see Fig. 9—11).

Figure 3J—O shows effects of conditioning antidromic stimulation of the whole stalk of the facial nerve on the testing antidromic shock. The negative waves evoked by testing stimulus were still depressed almost completely at 2 msec time interval and partially recovered at 3 msec and almost completely at 4 msec (Fig. 3J—L). When the time interval between two shocks was increased further, the test responses were again depressed (Fig. 3M—O). The duration of the depression lasted up to around 80—100 msec with a maximum depression at around 30 msec (Fig. 3P). Similar analysis was applied to the PA, TZ and BL branch and the time course of depression of the test response to each nerve branch after initial recovery from the refractoriness is shown in Fig. 3P. Even though there were some differences in the amount and the period of the maximum depression, a general tendency in each nerve branch tested was that a period of secondary depression of the test responses occurred and the duration of the depression lasted from 50 msec to 80 msec.

Intracellularly Recorded Action Potentials from FN Neurons Activated Antidromically

Figure 4A shows an example of intracellular unitary action potentials following stimulation of the PA branch. The latency was 0.8 msec and the spike rose to its peak in around 0.5 msec with a spike duration of 1.2 msec. The total amplitude of the spike was 60 mV with an inflection on its rising phase at about 25 mV above the level of the resting membrane potential. The spike potential was followed by a period of spike-after-hyperpolarization. Figure 4B shows the action potentials recorded from the same neurons following stimulation of the genu of the facial nerve. Aside from the latency differences (0.4 msec v. s. 0.8 msec), general characteristics of the action potential were quite similar to those activated by the peripheral nerve branch. Figure 4C shows an example of intracellularly recorded action potential from another FN neuron in response to the genu stimulation. In this neuron the spike potential was succeeded by a long period of after-polarization (Fig. 4C, indicated by an arrow).

Refractoriness of the FN neurons were studied by a double shock technique (Fig. 4D—L). Figure 4D shows spike potentials activated by PA stimulation. With a decrease in time intervals between shocks around 3 msec (Fig. 4G), the inflection of the test spike became more prominent with a prolongation of the spike duration. At around 2 msec time interval, the blockage of the spike occurred at the inflection leaving only the spike component of about 17 mV (Fig. 4F). At 1 msec time interval between shocks, this component could still be evoked (Fig. 4E). Figure 4H—J show another example of spike potentials tested by a double shock applied to the genu of the facial nerve. Changes in slope of the spike potentials with changes in shock intervals were fairly similar to the previous examples. Figure 4K and L show another FN neuron activated by a double shock stimulation of the genu of the facial nerve. In this neuron, the blocking at the inflection occurred at a time interval of around 2.5 msec between shocks

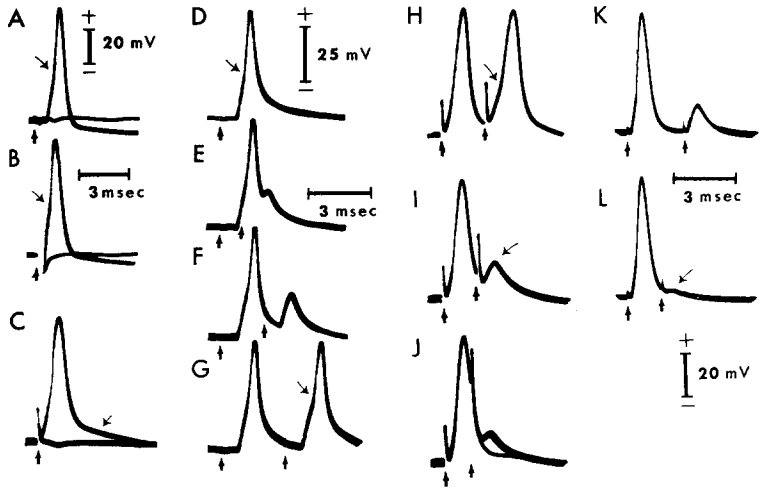

Fig. 4. *Intracellular recording of FN neurons responding to stimulation of PA* (A, D—G) or genu (B, C, H—L). A and B: recordings from one neuron to stimulation of PA or genu; C: spike potential with a pronounced after-depolarization indicated by down-going arrow. Stimulus strength in A, B and C was at threshold so that antidromic activation failed at about half of the trials. D—G: effects of double stimulation of PA branch. IS-SD inflection more pronounced with longer spike duration at 3 msec time interval (G), SD block at 2 msec (F). Effects of double shock stimulation of the genu recorded from one (H—J) and another (K—L) FN neuron. I: SD block and IS spike indicated by a down-going arrow noticeable at 1.5 msec time intervals; J: threshold of IS spike; K: SD block at 2.5 msec time interval; L: IS block and M spike noticeable indicated by a down-going arrow at 1.5 msec time interval. Time and voltage calibration of 3 msec and 20 mV in K—L refers also to H—J

leaving a spike component of about 12 mV (Fig. 4K). At 1.6 msec time interval, this spike was blocked completely, leaving only a small spike of about 2 mV to 3 mV in amplitude (Fig. 4L, indicated by down-going arrow). Judging from these results, in analogy to the antidromically activated spinal motoneurons (Brock *et al.*, 1953; Brock *et al.*, 1952; Coombs *et al.*, 1967). antidromic firing of the facial motoneurons is composed of three distinct membrane components, M, IS and SD spikes and hence, the sequence of antidromic invasion of spike potential to FN neurons is from the myelinated segment to the initial segment and finally to the soma-dendritic region.

Figure 5 illustrates variations in latencies of antidromic invasion of intracellularly recorded FN neurons activated from the peripheral nerve branches (50 units) and from the genu of the facial nerve (114 units). In some cases, the same neuron was activated by the peripheral as well as the genu stimulation. The latencies were measured from the onset of the stimulus to the initiation of the spike potentials. The latencies to the peripheral nerve branches (PA, TZ, BL) ranged from 0.46 msec to 1.1 msec with two peaks at around 0.6 msec and 0.8 msec. The latencies of the antidromic invasion from the genu ranged from 0.18 msec to 1.0 msec with two peaks around 0.3 msec to 0.4 msec and at around 0.6 msec to 0.7 msec. Aside from differences in conduction time between the peripheral nerve and genu stimulation, the overall patterns of distribution between the stimulation sites tested were very similar.

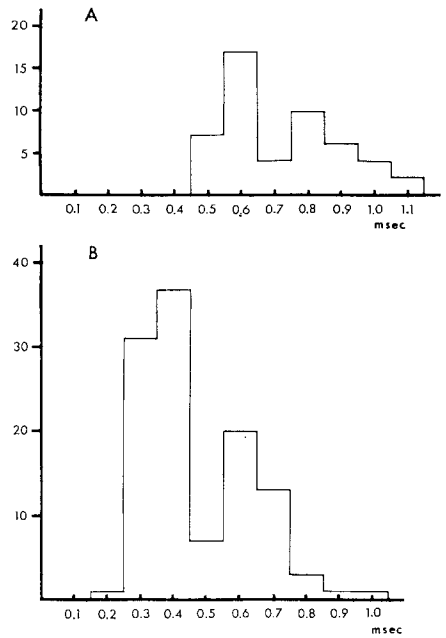

Fig. 5. *Histograms of latencies of antidromic spike potentials recorded intracellularly from FN neurons following stimulation of peripheral branches* (A) and of genu (B) of facial nerve. Ordinate: number of cells. Abscissa: latency in millisecond after the onset of stimulus. Note a close resemblance of the pattern of distribution of latencies between two histograms

In 36 neurons from which the resting membrane potentials were more than 45 mV and the spike amplitude of 50 mV to 90 mV, the rise time and falling time of the SD spikes were measured. The rise time was defined as being the onset of inflection to the peak of the spike potential and the fall time as from the peak of the spike potential to the point which intercepted the base line (see Fig. 6a, b, c). The rise time ranged from 0.23 msec to 0.53 with a mean of 0.37 msec (Fig. 6A) and the fall time ranged from 0.73 msec to 4.7 msec with a mean of 1.36 msec. As can be seen from Fig. 6B, the duration of the falling phase of the spike potentials varied much more widely than that of the rising phase. The wide variation was due mainly to those neurons with almost no appreciable spike-after-depolarization (Fig. 6Bb; Fig. 4A) and those with a relatively long spike-after-depolarization (Fig. 6Bc; Fig. 4C and D).

Spike-After-Potential by Antidromic Activation of Peripheral Branches and the Genu of the Facial Nerve

Samples of antidromically activated spike and spike-after-hyperpolarization are shown in Fig. 7A—J. The falling phase of spike potentials of FN neurons activated either by peripheral nerve branch or genu stimulation were of two types, one passing over into the after-hyperpolarization (Fig. 7C) and the other interrupted by positive potentials before passing into the after-hyperpolarization period (Fig. 7D). In all the FN neurons investigated at a threshold of intensity for spike potentials, we have failed to detect any synaptic potentials indicating an

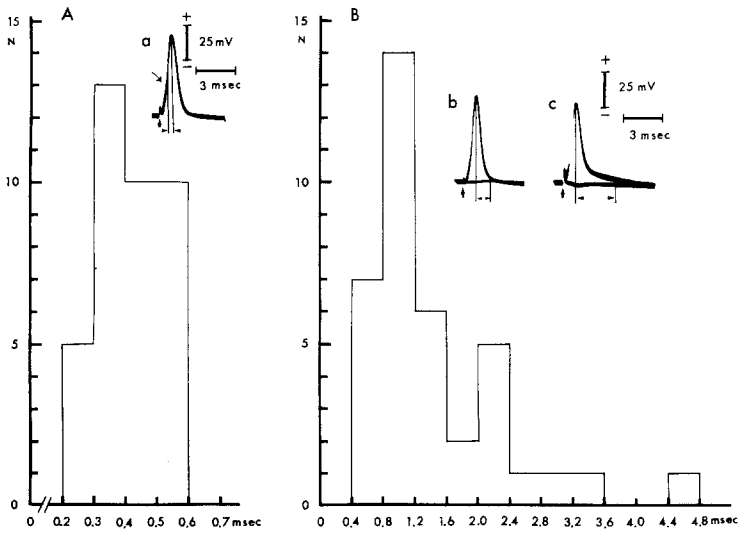

Fig. 6. *A: histogram of the rise time of SD spike antidromically activated.* Ordinate: number of cells. Abscissa: rise time in milliseconds. Rise time was defined from the point of IS-SD inflection to the peak and illustrated in a figure Aa. Down-going arrow indicated as IS-SD inflection and two vertical lines signified by horizontal arrows at the bottom was taken as rise time. B: histogram of the fall time of antidromically activated spike potentials. Ordinate: number of cells. Abscissa: fall time in milliseconds. Fall time was defined from the peak of spike to the point where the potential crossed the baseline. Sample records are illustrated in Bb and c. Distance between two vertical lines signified by arrows at the bottom in each figure was taken as fall time

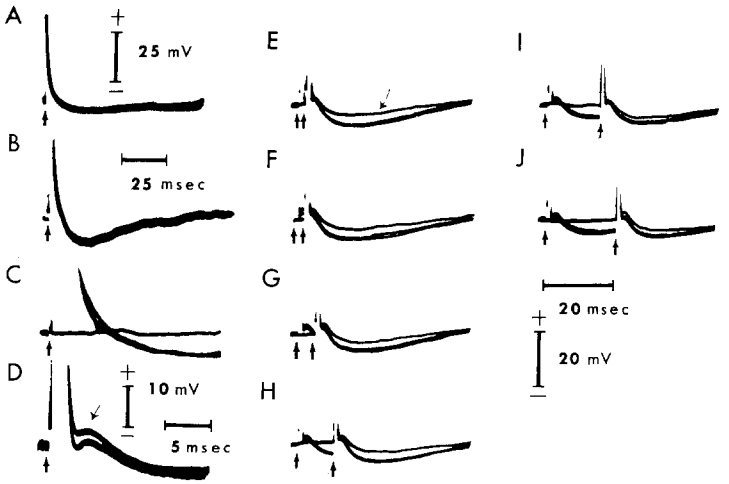

Fig. 7. *A: intracellular d—c recording and B: a—c recording showing spikes and after-potentials recorded from a FN neuron.* C: after-hyperpolarization without and D: with an interposed positive potential indicated by a down-going arrow recorded from two different cells. (The voltage calibration of 10 mV applies to B—D.) E—J: spike and after-hyperpolarization induced by double shock technique with varying time intervals between shocks. Control test responses indicated by a down-going arrow in E are superimposed with test responses when preceeded by a conditioning volley. Note a summation of after-hyperpolarization at short time intervals (E—H). Marked reduction of summation is seen with longer time interval between conditioning and test shocks (I—J)

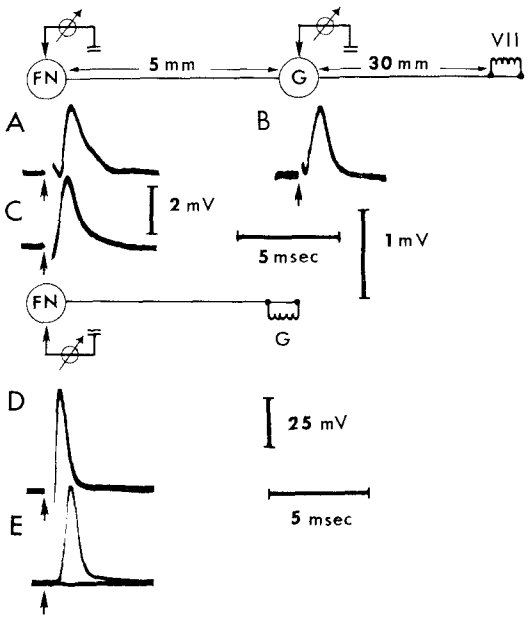

Fig. 8. *Diagramatic representations of stimulation and recording sites.* Numbers 5 mm and 30 mm in the diagram refer to approximated conduction distance from the genu (G) to FN and from the peripheral site (VII) to G. A: field potentials recorded in FN to VII stimulation; B: compound nerve potential to VII stimulation recorded at genu; C: field potentials in FN to G stimulation; D—E: action potential recorded from an impaled FN neuron to stimulation of VII and G

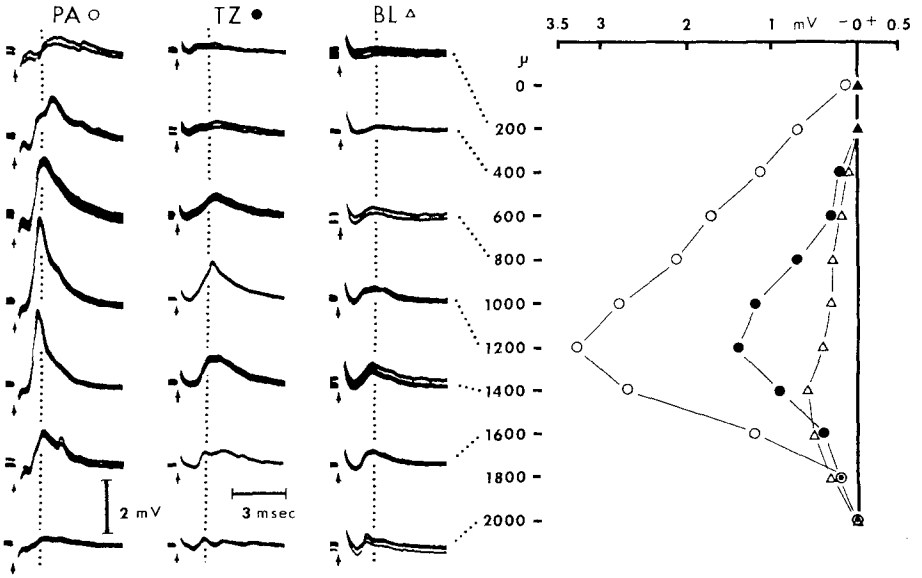

Fig. 9. *The depth profiles of PA, TZ and BL evoked field potentials recorded at the indicated depths in the medial portion of the FN.* The amplitudes and polarity of antidromic field potentials measured at the dotted vertical line in depth profile for PA (open circle), TZ (closed circle) and BL (open triangle) against the indicated depth. PA response is largest among three branches tested and reach a maximum at 1200 μ

absence of recurrent collateral pathway. The onset of the after-hyperpolarization was defined as the point at which the potentials intercepted the base line and the duration was measured from the onset to the point of potentials restoring to the base line. The amplitude was measured from the base line to the peak of the negative potential. Of 20 neurons analyzed with spike potential of more than 45 mV, it was found that the latencies to peak from the onset varied from 1.5 msec to 14 msec (mean and SD, 7.3 msec $\pm$ 3.6 msec, n = 20). The duration ranged from 6 msec to 60 msec (mean and SD, 31 msec $\pm$ 17 msec, n = 13). Only two neurons had duration of after-hyperpolarization longer than 50 msec and most common was a duration of around 30 msec to 40 mesc. The minimum amplitude of the after-hyperpolarization was 2 mV and maximum of 12 mV (mean and SD, 3.7 mV, $\pm$ 2.6 mV, n = 19).

Figure 7E—J illustrates the summation effects of after-hyperpolarization produced by a double shock applied to the genu of the facial nerve with various time intervals between shocks. When preceeded by the conditioning shock with short time intervals, the amplitudes of the test responses were almost twice as large as the control responses (Fig. 7E—H). The summation effects were decreased with increases in stimulus intervals between shocks and almost disappeared at around 15 or 20 msec time intervals.

Conduction Velocity

Conduction velocity of the axons of the facial motoneurons was examined by following manners: (A) Extracellular potential analysis. As illustrated in Fig. 8A and B, the entire stalk of the facial nerve was stimulated distal to the stylomastoid foramen and potentials were recorded simultaneously from the genu of the facial nerve and from the nucleus. As a control, the genu was stimulated through the recording electrode and the field potentials were recorded (Fig. 8C) from the same site as in Fig. 8A. (B) Intracellular spike potential analysis. Spike potentials were recorded intracellularly from the same FN neuron following stimulation of the genu and the peripheral facial nerve branches (see Fig. 4A, B and Fig. 8D, E). The conduction distance from the peripheral site to the genu was always about 30 mm to 32 mm and from the genu to the FN about 4 mm to 5 mm. The conduction velocity ranged from 42 m/sec to 100 m/sec for the peripheral portion (peripheral site to the genu) and 7 m/sec to 30 m/sec for the central portion (genu to FN) of the axons. The conduction velocity from the peripheral site to the FN ranged from 25 m/sec to 75 m/sec.

Topographical Representation of the Peripheral Branches of the Facial Nerve in the FN

Topographical representations of the PA, TZ, BL branches of the facial nerve in the FN were systematically analyzed by field tracking methods. Figures 9—11 show samples from such a study. The electrode tracts for each penetration were shown in Fig. 2. All these records were obtained from one animal under the same experimental conditions. The topographical depth analysis was done from the medial portion of the nucleus (Fig. 2B) to the intermediate (Fig. 2C) and to the lateral (Fig. 2D) portion. Though not shown, topographical depth analysis were done in the cephalocaudal direction as well and the findings were similar to those described below.

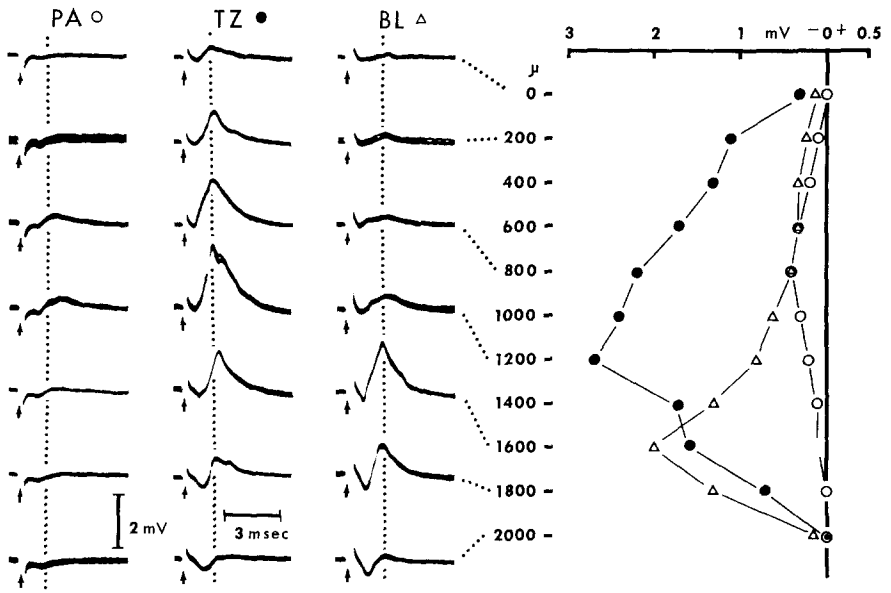

Fig. 10. *The depth profile of PA, TZ and BL evoked field potentials recorded at the indicated depths in the intermediate portion* (750 μ lateral to the penetration n Fig. 9) of the FN. Similar graphical representation was done as described in Fig. 9. Note much diminished PA responses and increased TZ and BL responses. TZ responses reach a maximum at 1200 μ and BL at 1600 μ

In the medial portion of the FN (Fig. 2B), the largest antidromic field potentials were produced by PA stimulation and were best developed at around 800 μ to 1400 μ (Fig. 9). In general, the antidromic field potentials evoked by PA stimulation had relatively simpler but always the largest negativity while configuration of potentials evoked by TZ or BL were more complex. The potentials evoked by TZ or BL branches were much smaller in amplitudes and less synchronized in the medial portion of the nucleus. However, it could be seen that the TZ responses were slightly better developed and more dorsally represented than the BL responses.

Figure 10 illustrates recordings obtained from the intermediate portion of the FN (Fig. 2C). Even though there was only a separation of about 750 μ from the medial tract, the PA responses were almost completely absent in this area. Instead, relatively large potentials were evoked in the middle portion of the nucleus (800 μ to 1200 μ) following TZ stimulation and in the ventral portion (1600 μ to 1800 μ) following BL stimulation with slight dominance in responsiveness to the TZ stimulation over BL stimulation.

Moving laterally (Fig. 2D) by about 500 μ from the intermediate tract, it was found that no potential could be recorded by PA stimulation (Fig. 11). Though smaller in the amplitudes compared to the previous tract (Fig. 10), both TZ and BL responses were still detected with TZ responses appearing more dorsal to the BL responses. In this area, however, the BL responses were as strongly represented as TZ responses. Also noted was that the depolarization of the FN neurons was

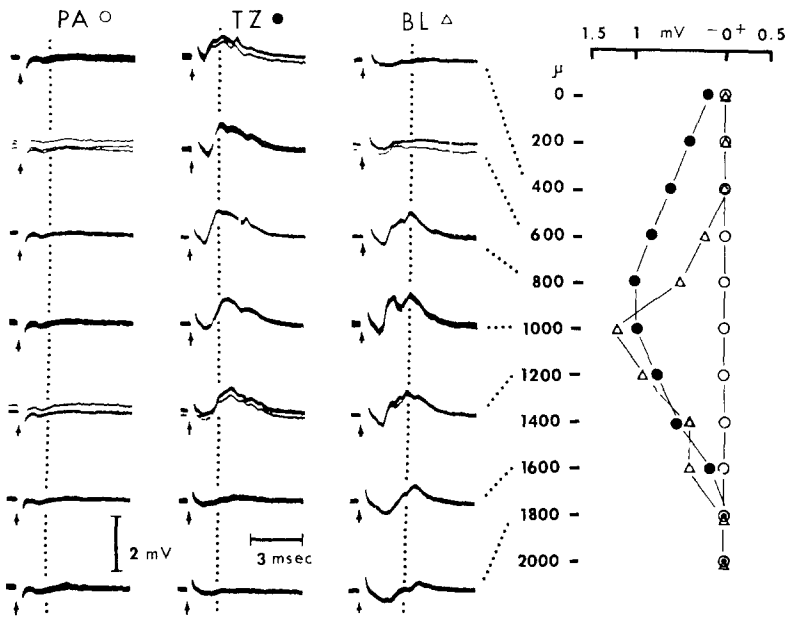

Fig. 11. *The depth profile of PA, TZ and BL evoked field potentials recorded at the indicated depth in the lateral portion* (500 μ lateral to the penetration of Fig. 10) of the FN. Graphical representation of the changes in amplitudes of field potentials similarily constructed as in Fig. 9 is shown. Note no PA responses recorded in this area. Both TZ and BL responses are still recorded with slight predominance of BL over TZ responses. Note also that the over-all representation of BL responses is ventral to that of TZ responses

much less synchronized (especially in BL) without appreciable changes in latencies or the total duration of the negative waves.

Synaptic Inputs to the FN Following Peripheral Nerve Stimulation

When peripheral branches of the facial nerve were stimulated, it was observed in the FN that second negative potentials were evoked succeeding the well synchronized short latency antidromically activated potentials. The second negative potentials usually had latencies of 4 msec to 7 msec, the duration of approximately 10 msec and the amplitude about $^1/_3$ of that of antidromic potentials. To identify that these second negative waves were evoked by the synaptic inputs, their graded nature by stimulus intensity change, summation effect and refractoriness were tested and intracellular analysis performed.

Figure 12A—E show the effects of progressive changes of stimulus intensity. At the stimulus intensity 1.5 or 2 times the threshold of the antidromic potentials (first negative waves), no succeeding waves were evoked. Small amplitude negative waves (Fig. 12C, indicated by down-going arrow) were noticed at the stimulus intensity 3 times the threshold. With a further increase in the stimulus intensities, the amplitude and duration of the second negative waves increased with some decrease in their latencies (Fig. 12D, E).

Figure 12F—I demonstrate effects of a double shock applied to the PA with varying time intervals between shocks. With a time interval of 1 msec (Fig. 12G),

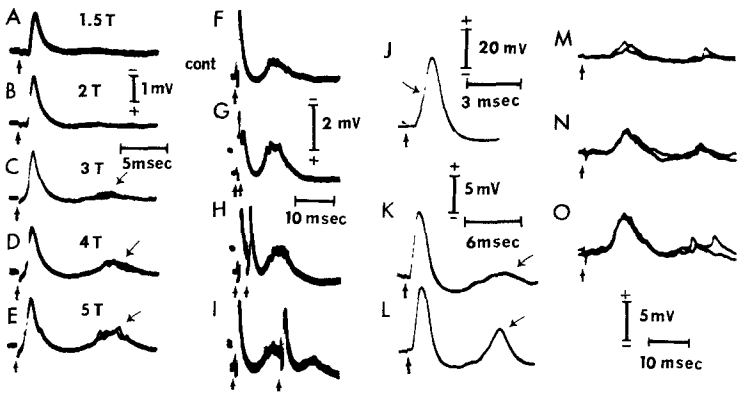

Fig. 12. *A—E: field potentials produced by PA stimulation with varying stimulus intensities recorded in the FN.* Numbers on the upper right hand of each record refer to the stimulus intensity relative to the threshold of the initial negativity (antidromic responses). Second negativity is detectable with stimulus strength at 3T (C) indicated by a down-going arrow. The amplitude of the second negativity increases with increase in stimulus intensity (C—D). F—I: testing of PA evoked field potentials by a preceeding PA conditioning volley at various time intervals between conditioning and testing shock. F: control test response. G: at 1 msec shock interval, note a reduction of antidromic test response and increase of second negativity when preceeded by a conditioning shock. H: at 3 msec time interval, note a recovery of antidromic test response while second test negativity is still increased from the control test response. I: at 12 msec shock interval. Note the antidromic test response is occluded when temporally coincided with the conditioning second negative wave. Note also a reduction of second test response at this time interval. J—O: intracellular recording from FN neurons following stimulation of facial nerve. J: antidromically activated action potential (downward-going arrow indicates IS-SD inflection). K—L: recordings from the same neuron as C except with higher CRO gain and slower sweep. Short latency IS spikes followed by EPSPs indicated by downward arrow. Increase in the amplitude of EPSPs with increase in stimulus intensity from K—L. M—O: EPSPs recorded from another neuron. Increase in the amplitude of EPSPs with a gradual increase in the stimulus intensities from M to O. Note also an enhancement of late EPSPs from M to O

the initial antidromically activated potentials were still in their refractoriness. However, the amplitudes and the duration of the second negative waves became much larger when compared with the control test response (Fig. 12F). At 3 msec time interval between shocks (Fig. 12H), the antidromic test responses were no longer suppressed by the preceeding conditioning shock but the second negative waves still summated. At 12 msec time intervals, the antidromic potentials were occluded when they temporally coincided with the second negative wave of the conditioning response. At the same time, the second negative waves evoked by test stimulus were partially at their refractory period. Figure 12J shows an intercellularly recorded antidromic spike from a FN neuron following stimulation of the PA branch. The action potential had a latency of 0.5 msec with an IS-SD inflection and an after-hyperpolarization. Figure 12K and L show recordings from the same neuron activated with reduced stimulus intensities and recorded with a slower time sweep and higher gain of the oscilloscope. In this recording, the antidromic invasion failed to evoke a full action potential but only an IS spike. This spike had a latency of 0.5 msec and the duration of 2 msec followed by a

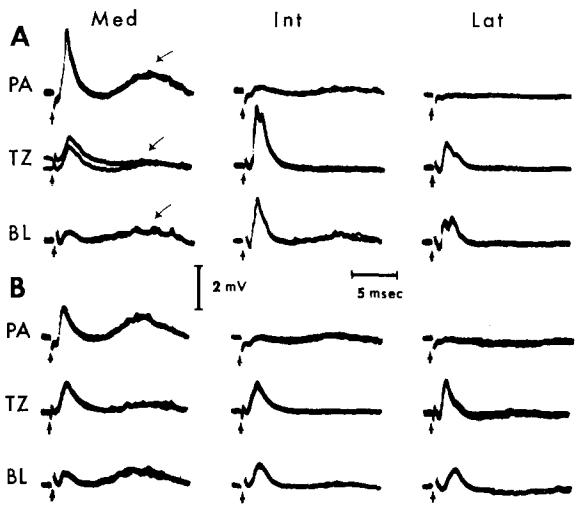

Fig. 13. *A: topographical analysis of antidromic field potentials following PA*, TZ, BL stimulation in the medial (Med), intermediate (Int) and lateral (Lat) portions of the FN. Separation of 750 μ between Med and Int and 500 μ between Int and Lat. In each penetration, PA, TZ, BL responses were recorded from a same site. Antidromic action potentials are succeeded by second negative waves indicated by down-going arrows. Largest second negative waves are observed in the Med penetration and PA stimulation. B: similar topographical analysis as in A except recordings were obtained 500 μ rostral in FN from A

small hyperpolarization. This hyperpolarization was interrupted by a later depolarization (latency of 5 msec from the onset of stimulus with a peak amplitude of 2.5 mV) (Fig. 12K). With an increase in stimulus intensity, the amplitude of the late depolarization was increased (Fig. 12L). Figure 12M—O show EPSPs recorded from another FN neuron following stimulation of the BL branch. Though the neuron was identified as an FN neuron by antidromic activation, the antidromic spike potential was not triggered at these levels of stimulus intensity. With a weak stimulation, EPSPs with a latency of 7 msec and a duration of 8 msec and small later EPSPs were induced (Fig. 12M). With increase in stimulus intensity, the latency of the onset of the EPSPs became shorter and their duration and amplitudes increased (Fig. 12N—O). The late EPSPs with latencies of 20 msec to 25 msec also became more apparent and their latency decreased.

A topographical representation of these synaptic inputs in the FN was tested by systematic field potential tracking in various loci in the FN following stimulation of PA, TZ and BL branches of facial nerve. Figure 13A shows field potentials activated by various branches and recorded at three locations (medial, intermediate and lateral portions) in the FN with separation of 750 μ between medial to intermediate and 500 μ between intermediate to lateral electrode tract. In the medial portion of the nucleus, the PA stimulation evoked a relatively large synaptically activated field potential (Fig. 13A, PA indicated by down-going arrow) preceeded by antidromically activated potentials. Even though the TZ and BL stimulation failed to evoke a large antidromic response, small synaptically activated potentials (especially by the BL stimulation) were observed. In the

intermediate portion, small synaptically activated potentials were still recorded to stimulation of PA and BL but not to TZ (though the TZ stimulation evoked a large antidromic potential). In the lateral portion of the FN, no synaptic responses were observed. In Fig. 13B, recording electrodes were moved one millimeter rostral to the previous antero-posterior coordinate and similar medial-to-lateral analysis were performed. In general, the antidromic responses to all the branches stimulated were much smaller in amplitude. However, relatively large synaptically activated field potentials were detected in the medial portion of the nucleus. These analyses indicate that the afferent inputs from the peripheral branches of facial nerve tested are terminating mainly in the medial aspect of the nucleus. Also noted was that the largest synaptic inputs were produced by the PA branch of the facial nerve.

Discussion

Field Potentials Induced by Antidromic Activation

When the recording electrode tip was within the FN, stimulation of either the peripheral branches or the genu of the facial nerve resulted in production of clearly defined negative field potentials. These negative potentials were identified as the summated action currents in the FN neurons resulting from antidromic invasion. The identifications were based on several criteria: (1) a graded nature of the negativities with changes in the stimulus intensities; (2) a brief latency of less than 1 msec; (3) short refractory period of 2—3 msec; (4) a relatively short duration of the negative waves; (5) relative correspondence of the intracellularly recorded antidromic unitary action potentials with the time course of the negative waves and (6) the location of the large negative waves recorded corresponded to the soma of the FN neurons.

In general, the antidromic field potentials had some inflexions on the falling phase of the negative wave signalling some differences in a rate of depolarization of a large number of neurons. As will be discussed in conduction velocities of the FN neurons, the diameters of the axons and the soma of the FN neurons vary fairly widely (Foley and DuBois, 1943; VanBuskirk, 1945) which could account for the above phenomena. It was observed in some penetrations, that these negative field potentials were preceeded by a small positive wave with a latency of 0.5 msec. Also, as the electrode was at or nearing the ventral limit of the nucleus (as identified from a histological correlates), the amplitude of the negative waves decreased and became clearly diphasic (positive-negative) and in many cases, reversed to a small positivity. Histological findings (Ramón y Cajal, 1909) show that organization of the FN is such that the axons of the FN neurons are mainly directed dorso-medially and the dendrite ventrolaterally in the nucleus. The initial positive wave with a brief latency of around 0.5 msec could be interpreted as the incoming invasion volley along the axons of the FN and the succeeding negative wave as antidromic invasion to the soma. The reversal of the negative waves to the positive could be due to the fact that the antidromic action potentials in the FN neurons do not invade the total extent of the dendrites. The present depth profile analysis revealed, therefore, that the field organization in the FN is similar to that observed in other cranial motor nuclei (Baker and Precht, 1972; Lorente de Nó, 1935; Porter, 1968; Sasaki, 1963).

During double shock testing of the antidromic responses, the test responses were suppressed (after initial recovery from the refractory period) for a duration of around 50 msec to 100 msec with a maximum suppression at around 20 msec to 30 msec. This suppression could not be attributed entirely to the effects of spike after-hyperpolarization since intracellular analysis revealed that the duration of the spike after-hyperpolarization was usually less than 40 msec. It was also noted that in some neurons action potentials could be triggered during after-hyperpolarization period. The suppression may partially be due to the occlusion with the synaptic inputs observed in the present study. However, a presence of some inhibitory mechanisms could not be dismissed since IPSPs were detected in some FN neurons following stimulation of spinal trigeminal nucleus (Iwata *et al.*, 1972).

On the other hand, we have failed to detect clearly identifiable IPSPs from the FN neurons following antidromic activation. The recurrent axon collateral activation has not been established in other cranial motor nuclei (Baker and Precht, 1972; Porter, 1965; Sasaki, 1963) while much interaction between motoneurons by their axon collateral pathways was found in the spinal cord (Eccles *et al.*, 1954). It was reported that the trochlear or abducence (Baker and Precht, 1972) and hypoglossal motoneurons (Porter, 1968) can modify their excitability by spike after-hyperpolarization even in the absence of any collateral pathways. It is possible to consider that an apparent lack of collateral inhibition coupled with a relatively shorter spike after-hyperpolarization in the FN and other cranial motoneurons suggests a difference in functional property of the muscles by which the cranial motoneurons control. In the oculomotor nuclei which controls a short twitch duration of the extrinsic eye muscle, much higher tonic discharges were detected in the oculomotor neurons as compared to the lumbar spinal motoneurons (Sasaki, 1963). In the FN, we have failed to detect much spontaneous tonic discharge of the FN neurons. It was more common to see their discharge pattern in a form of a burst response especially when excited by synaptic inputs (Tanaka *et al.*, 1971).

Intracellularly Recorded Action Potentials From FN Neurons Activated Antidromically

Antidromic firing of the facial motoneurons is quite similar to other CNS neurons (Brock *et al.*, 1953; Brock *et al.*, 1952; Coombs *et al.*, 1957; Eccles *et al.*, 1958; Ito *et al.*, 1964; Kuno ,1959; Porter, 1968; Sasaki, 1963; Tsukahara *et al.*, 1967), and is composed of three distinct membrane components, M-, IS- and SD-spike (Brock *et al.*, 1953; Coombs *et al.*, 1957). The time course of the action potential resembled that of oculomotor (Sasaki, 1963), hypoglossal (Porter, 1968) and spinal motoneurons (Brock *et al.*, 1952). The rise time of 0.37 msec is quite similar to the hypoglossal neurons (0.5 msec) (Porter, 1968) and the Deiters neurons (Ito *et al.*, 1964). The fall time of the SD spike ranged from 0.73 msec to 4.7 msec with a mean of 1.36 msec. However, closer examination of the distribution of the fall time reveals two types of neurons, one having no appreciable spike after-depolarization (Fig. 6Bb) and the other a relatively long spike after-depolarization (Fig. 6Bc). One can group one type of neurons having fall time of 0.4 msec to 1.5 msec and the other over 1.6 msec to about 4 msec. One group

with shorter fall time (0.4 msec to 1.5 msec) is comparable with the spinal motoneurons (Eccles *et al.*, 1958) and other with the hypoglossal motoneurons which also show a prolonged period of membrane depolarization (Porter, 1968). The facial motoneurons, therefore, are of both slow (fall time of approximately 1 msec to 1.2 msec) and fast (less than 1 msec) type of motoneurons differentiated in their functional characteristic (Eccles *et al.*, 1958). It is also interesting to know that these neurons with long after-depolarization, when synaptically activated, tended to fire all-or-none burst of spikes with concomitant all-or-none large depolarizing potentials (Tanaka *et al.*, 1971).

As in other motoneurons, the after-hyperpolarization follows the termination of spike potential. The time course of after-hyperpolarization of 31 msec (range 6 msec to 60 msec) in FN neurons was like that of the oculomotor (Sasaki, 1963) or trochlear (Baker and Precht, 1972) neurons and much shorter than the spinal motoneurons (50 msec to 180 msec) (Eccles *et al.*, 1958). The summit time of the after-hyperpolarization of 1.4 msec to 14 msec, however, was comparable more to spinal motoneurons (6 msec to 15 msec) (Brock *et al.*, 1952; Eccles *et al.*, 1958; Kuno, 1959) than to Deiters neurons (0.7 msec to 2.7 msec) (Ito *et al.*, 1964) or red nucleus neuron (1.4 msec to 3.0 msec) (Tsukahara *et al.*, 1967). A similarity also noted between the facial motoneurons and the spinal motoneurons is the pattern of summation of after-hyperpolarization when induced by a double shock with varying time intervals. As in the spinal motoneurons (Ito *et al.*, 1962), the summation effect was larger at shorter time intervals. The effect of the conditioning lasted much shorter in duration in the facial motoneurons (about 20 msec) than in the spinal motoneurons (60 msec to 70 msec) (Ito *et al.*, 1962) and this may reflect the shorter time course of the spike after-hyperpolarization observed in the facial motoneurons.

Conduction Velocities

According to VanBuskirk (1945), facial nerve in cats were mostly myelinated (80%) and the fiber size measured at the peripheral portion ranged from 1.5 μ to 14 μ with the majority around 3 μ and 6 μ. The observations by others (Bruesch, 1944; Foley and Du Bois, 1943) are also in general agreement with the above findings. These wide variations in fiber spectrum are also reflected on the variation of the conduction velocities (25 m/sec to 75 m/sec) observed. Differences were found in the conduction velocities between the peripheral portion (42 m/sec to 100 m/sec) and the central portion (7 m/sec to 30 m/sec). These discrepancies could be attributed partially to the assessment of the exact distance from the point of genu stimulation to the recording site. Since the FN lies caudal to the level of the genu of the facial nerve and the nerve curves in its course to the nucleus, the straight line of distance measured from the genu to the facial nucleus will result in underestimation of the conduction distance. Also the latency for initiating impulses at the very site of the stimulation would lead to an overestimation of the conduction time. Thus, the velocity will be slightly faster than actually calculated. Another reason for some discrepancy may be that the exact assessment of the latencies becomes much more critical for the measurement of conduction velocity for the central portion compared to the peripheral since the conduction distance is much shorter (5 mm v. s. 30 mm) for the former. Other

reasons may arise from structural differences between the peripheral (or extra-medullary) and the central (or intra-medullary) portion of the axons and also to the functional differences. Even considering these difficulties, the conduction velocities (25 m/sec to 75 m/sec) found in the present study show a greater range of variation than the velocity of about 50 m/sec reported by Lindquist (1970) but are much more similar to those of occulomotor nerves (30 m/sec to 80 m/sec) (Sasaki, 1963) and hypoglossal nerves (24 m/sec to 60 m/sec) (Porter, 1968).

Topographical Representation

Topographical representation of the peripheral branches of facial nerve revealed by field potential analysis was that the PA was represented solely in the medial aspect, TZ mainly in the dorsal aspect of the intermediate portion and BL in the ventral aspect of the intermediate and mainly in the lateral aspect of the FN. These findings are in agreement with anatomical findings by Courville (1966) and to a great deal with those of Papez (1927) and Vraa-Jensen (1942). The anatomical studies also showed that the intermediate group is located more dorsally, while the lateral group lies in ventro-medial axis and the ventral portion of the lateral group is located immediately ventral to the intermediate group (Courville, 1966; Vraa-Jensen, 1942). This overlap of the intermediate and the lateral group in a direct dorso-ventral position (as the recording electrode penetrated) in the nucleus will account for the findings that the TZ evoked field potentials were recorded in the dorsal aspect of the intermediate portion of the nucleus (Fig. 2C and Fig. 10). Some overlapping of the TZ and BL responses recorded from the lateral portion of the nucleus (Fig. 2D and Fig. 11) could also be due to the fact that greater portions of the lateral group lies ventrally to the intermediate group. On the other hand, the dorsomedial groups is well-circumscribed and lies medially in the nucleus, thus the potentials evoked by PA stimulation were detected only in the medial aspect (Fig. 2B and Fig. 9). In the present field potential analysis, it was found that the PA evoked potentials were generally much larger than the other two branches investigated. Anatomical findings (Courville, 1966; Vraa-Jensen, 1942) showed that the medial group was most prominent in cats (Courville, 1966), as well as in dogs (Vraa-Jensen, 1942), while the lateral group was very prominent in the human (Vraa-Jensen, 1942) and the medial group insignificant. These findings suggest the existence of functional correlation of the mimetic role of buccolabial muscles in man and the importance of auricular musculature in lower animals. The present electrophysiological findings support this notion.

Synaptic Inputs from the Peripheral Nerve Stimulation

Some synaptic phenomena produced in the FN following stimulation of the ipsilateral perpheral nerve was detected by intra- and extra-cellular recording technique. The latencies of both field potentials and EPSPs were around 4 msec to 7 msec from the onset of the stimulation. Anatomical studies (Bruesch, 1944; Foley and DuBois, 1943; VanBuskirk, 1945) demonstrated that in cat, about 12—15% of the facial nerve distal to the stylomastoid foramen are sensory fibers whose cell bodies are located in the geniculate ganglion and the innervate mainly or solely to the auricular region and to some extent the mimetic musculature.

Though the exact functional nature of these sensory fibers is not completely agreed upon among investigators, behavioral observations have indicated some loss of pressure and pain (Davis, 1923) and proprioception sense (Carmichael, 1933) over the face in man and in aminal due to the disturbance of the facial nerve. In the study of blink reflex in cats, Lindquist and Martenson (1970) demonstrated that the facial nerve contains high-threshold afferent fibers and suggested that they may be activated from extroceptive receptors. Anatomical study (Bruesch, 1944) showed that afferent fibers terminate as free endings in the adventitia of blood vessels in the facial area. These sensory fibers are relatively small (1.5—6.5 μ; majority, 2.5—3.5 μ). The central termination of these afferent components of the facial nerve is in the gray associated with the fasiculus solitarius or in the nucleus of the spinal tract of the trigeminal (Crosby *et al.*, 1962; Rhoton, Jr., 1968).

The trigemino facial projections are either via collaterals of secondary trigemino-thalamic tract (Mogami *et al.*, 1968; Ramón y Cajal, 1909) or from direct trigemino-facial fibers (Carpenter and Hanna, 1961; Stewart and King, 1963). A di- or poly-synaptic activation (2 msec to 3 msec latency) of facial motoneurons following stimulation of the trigeminal nerve and a monosynaptic activation (0.8 msec to 1.5 msec latency) of facial motoneurons by thalamic (VPM) or trigeminal nucleus stimulation have been observed by an intracellular analysis (Tanaka *et al.*, 1971; Christensen *et al.*, 1972). Monosynaptic field and unitary potentials were also detected in the spinal trigeminal nucleus following facial nerve stimulation (Iwata *et al.*, 1972). These anatomical and physiological observations could account for the presently found synaptic excitation of the FN neurons following stimulation of the peripheral branches of the facial nerve. A predominant representation of synaptic inputs in the medial aspects of the nucleus by PA stimulation and a relative lack of synaptic inputs from the TZ branch are also in accord with the anatomical findings (Bruesch, 1944; Foley and DuBois, 1943; Vraa-Jensen, 1942).

The authors express their gratitude to Mrs. D. Agresta for her patient and skillful assistance in histology and photography and to Dr. J. F. DeFrance and T. Weilepp for their comments and advice in the preparation of this manuscript. Thanks are also due to Drs. T. Akaike, T. Bando and K. Hatada for their assistance in the preliminary portion of this experimentation.

References

Baker, R., Precht, W.: Electrophysiological properties of trochlear motoneurons as revealed by IVth nerve stimulation. Exp. Brain Res. **14**, 127—157 (1972).

Brock, L.G., Coombs, J.S., Eccles, J.C.: Intracellular recording for antidromically activated motoneurons. J. Physiol. (Lond.) **122**, 429—461 (1953).

— — — The recording of potentials from motoneurons with an intracellular electrode. J. Physiol. (Lond.) **117**, 431—460 (1952).

Bruesch, S.R.: The distribution of myelinated afferent fibers in the branches of the cat's facial nerve. J. comp. Neurol. **81**, 169—191 (1944).

Carmichael, E.A., Woollard, H.H.: Some observations on the fifth and seventh cranial nerves. Brain **56**, 109—125 (1933).

Carpenter, M.B., Hanna, G.R.: Fiber projections from the spinal trigeminal nucleus in the cat. J. comp. Neurol. **117**, 117—125 (1961).

Christensen, C., Iwata, N., Kitai, S.T.: Trigemino-facial relationships in cat: A microelectrode study. Anat. Rec. **172**, 289 (1972).

Coombs, J.S., Curtis, D.R., Eccles, J.C.: The interpretation of spike potentials of motoneurons. J. Physiol. (Lond.) **139**, 198—231 (1957).

Courville, J.: The nucleus of the facial nerve; the relation between cellular groups and peripheral branches of the nerve. Brain Res. **1**, 338—354 (1966).

Crosby, E.C., Humphrey, T., Lauer, E.W.: Correlative Anatomy of the Nervous System. New York: MacMillan Co. 1962.

Davis, L.E.: The deep sensibility of the face. Arch. Neurol. Psychiat. (Chic.) **9**, 283—305 (1923).

Eccles, J.C., Eccles, R.M., Lundberg, A.: The action potentials of the alpha motoneurons supplying fast and slow muscles. J. Physiol. (Lond.) **142**, 275—291 (1958).

— Fatt, P., Koketsu, K.: Cholinergic and inhibitory synapses in a pathway from motor-axon collaterals to motoneurons. J. Physiol. (Lond.) **126**, 524—562 (1954).

Foley, J.O., DuBois, F.S.: An experimental study of the facial nerve. J. comp. Neurol. **79**, 79—105 (1943).

Huber, E., Hughson, W.: Experimental studies on the voluntary motor innervation of the facial musculature. J. comp. Neurol. **42**, 113—163 (1926).

Ito, M., Hongo, T., Yoshida, M., Okada, Y., Obata, K.: Antidromic and trans-synaptic activation of Deiters' neurones induced from the spinal cord. Jap. J. Physiol. **14**, 638—658 (1964).

— Oshima, T.: Temporal summation of after-hyperpolarization following a motoneurone spike. Nature (Lond.) **195**, 910—911 (1962).

Iwata, N., Kitai, S.T., Olson, S.: Afferent component of the facial nerve: Its relation to the spinal trigeminal and facial nucleus. Brain Res. (In Press).

Kitai, S.T., Bando, T., Tanaka, T., Tsukahara, N., Yu, H.: Antidromic activation of the facial motor neuron in cat. Brain Res. **33**, 227—232 (1971).

Kugelberg, E.: Facial reflexes. Brain **75**, 385—396 (1952).

Kuno, M.: Excitability following antidromic activation in spinal motoneurones supplying red muscles. J. Physiol. (Lond.) **149**, 374—393 (1959).

Langworth, E.P., Taverner, D.: The prognosis in facial palsy. Brain **86**, 465—480 (1963).

Lindquist, C.: Microelectrode recording from the facial nucleus in the cat. Acta physiol. scand. **80**, 1A—2A (1970).

— Martensson, A.: Mechanisms involved in the cat's blink reflex. Acta physiol. scand. **80**, 149—159 (1970).

Lorente de Nó, R.: The synaptic delay of the motoneurones. Amer. J. Physiol. **3**, 272—282 (1935).

Mogami, H., Kuroda, R., Hayakawa, T., Kanai, N., Yamada, R.: Ascending pathways from nucleus caudalis of spinal trigeminal nucleus in cat — with special reference to pain conduction pathway. Med. J. Osaka Univ. **19**, 49—70 (1968).

Papez, J.W.: Subdivisions of the facial nucleus. J. comp. Neurol. **43**, 159—191 (1927).

Pearson, A.A.: The roots of the facial nerve in human embryos and fetuses. J. comp. Neurol. **87**, 139—159 (1947).

Porter, R.: Antidromic responses of hypoglossal motoneurons. Exp. Neurol. **20**, 624—634 (1968).

— Synaptic potentials in hypoglossal motoneurons. J. Physiol. (Lond.) **180**, 209—224 (1965).

Ramón y Cajal, S.: Histologie du Système Nerveux de l'Homme et des Vertébrés, pp. 859—888. Paris: Maloine 1909.

Rhinehart, D.A.: The nervus facialis of the albino mouse. J. comp. Neurol. **30**, 81—125 (1918).

Rhoton, A.L., Jr.: Afferent connections of the facial nerve. J. comp. Neurol. **133**, 89—100 (1968).

Sasaki, K.: Electrophysiological studies on oculomotor neurons of the cat. Jap. J. Physiol. **13**, 287—302 (1963).

Stewart, W.A., King, R.B.: Fiber projections from the nucleus caudalis of the spinal trigeminal nucleus. J. comp. Neurol. **121**, 271—286 (1963).

Szentágothai, J.: The representation of facial and scalp muscles in the facial nucleus. J. comp. Neurol. **88**, 207—220 (1948).

Tanaka, T., Yu, H., Kitai, S.T.: Trigemino and spinal inputs to the facial nucleus. Brain Res. **34**, 504—508 (1971).

Tsukahara, N., Toyama, K., Kosaka, K.: Electrical activity of red nucleus neurons investigated with intracellular microelectrodes. Exp. Brain Res. **4**, 18—33 (1967).
VanBuskirk, C.: The seventh nerve complex. J. comp. Neurol. **82**, 303—333 (1945).
Vraa-Jensen, G.F.: The Motor Nucleus of the Facial Nerve. With a Survey of the Efferent Innervation of the Facial Muscles. Copenhagen: Ejnar Munksgaard 1942.
Woody, C.D., Brozek, G.: Gross potential from facial nucleus of cat as an index of neural activity in response to glabella tap. J. Neurophysiol. **32**, 704—716 (1969).
— — Changes in evoked responses from facial nucleus of cat with conditioning and extinction of an eye blink. J. Neurophysiol. **32**, 717—726 (1969).
Yu, H., DeFrance, J.F., Iwata, N., Kitai, S.T., Tanaka, T.: Rubral inputs to the facial motoneurons in cat. Brain Res. **42**, 220—224 (1972).

S. T. Kitai
Morin Memorial Laboratory
Wayne State University
School of Medicine
Department of Anatomy
550 E. Canfield
Detroit, Michigan 48201
USA